An acoustic double fishnet using Helmholtz resonators

A. R. J. Murray,[a)] I. R. Summers, J. R. Sambles, and A. P. Hibbins

Electromagnetic and Acoustic Materials, Department of Physics and Astronomy, University of Exeter, Stocker Road, Exeter, EX4 4QL, United Kingdom

The acoustic transmission of a closely spaced pair of patterned and perforated rigid plates is explored in air. The structure resembles an acoustic double fishnet design, with each plate modified such that the gap between them acts as an array of Helmholtz resonators. This allows the center frequency of the stop band to be reduced by a factor greater than 2 from the value obtained for the conventional acoustic double fishnet design. Experimental results accord well with the predictions of a finite element model. © *2014 Acoustical Society of America*.
[http://dx.doi.org/10.1121/1.4892859]

I. INTRODUCTION

The discovery of extraordinary optical transmission (EOT) by Ebbesen,[1] often defined as a mechanism that facilitates a transmitted intensity greater than that predicted by Bethe's classical aperture theory,[2] has generated increased interest in the transmission properties of sub-wavelength periodic hole or slit arrays. The similarity between the governing equations of electromagnetism and acoustics has stimulated comparable work with sound waves. Unlike the electromagnetic case for periodic holes in a metal plate, holes in an acoustically rigid wall do not possess a cut-off frequency for plane-wave propagation and so enhanced transmission of sound through arrays of holes in a thick rigid screen is typically associated with the excitation of Fabry–Pérot-like resonances in the pipes.[3] However, there is a second mechanism that can also lead to enhanced transmission, which is somewhat more in keeping with the electromagnetic results of Ebbesen:[1] extraordinary acoustic transmission (EAT) is observed at wavelengths just longer than the pitch of the hole array due to the diffractive excitation of acoustic surface waves on both faces of the plate, that are coupled via the holes.[4] Another example of enhanced transmission, of a non-resonant nature, is the broadband transmission of sound at high angles of incidence due to geometric impedance matching.[5] In contrast to the EAT phenomena, Estrada *et al.*[6] found that there may be a band of complete reflection at wavelengths close to the periodicity of the hole array, in addition to the EAT phenomenon. Other studies have considered the combination of two rigid perforated plates separated by a small gap, termed the acoustic double fishnet (ADF), which possesses a family of acoustic stop bands[7,8] associated with the resonances of the gap. Acoustic screening and absorption by locally resonant acoustic materials (LRAMs) has also generated interest. Studies have considered the effect of LRAM inclusions within panels[9–11] to increase the transmission loss or porous materials[12,13] to increase absorption at frequencies around the resonances of the LRAMs. Other studies have considered the acoustic properties of arrays of cylinders with particular attention on the band-gaps they possess.[14–16] Many of these structures are promoted as providing lightweight sound screens tailored to desired frequency bands, the ADF is one such structure that simultaneously allows the flow of air through the screen. In our present work, we report on a modified ADF structure (Fig. 1) in which the frequency of the associated acoustic stop band in air is significantly lowered from that of the unstructured ADF.

II. HELMHOLTZ ACOUSTIC DOUBLE FISHNET

A conventional ADF is comprised of two identical rigid plates each perforated with a non-diffracting, square array of circular holes (with pitch Λ). The plates are aligned and separated by a sub-wavelength gap (with height h_g). As detailed in previous papers,[7,8,17] sound screening occurs around the frequency associated with the resonance of the gap; being determined primarily by the pitch of the hole array; although the gap height and hole alignment also influence the stop band frequency. As the present authors report elsewhere,[18] increasing either the height of the gap or the misalignment of the holes serves only to increase the frequency at which the stop band occurs. In order to reduce the frequency of the stop band, one can simply increase the pitch of the array. However, this can lead to unwanted diffraction and reduce the ratio of hole to solid. Instead, in the present study, we seek to reduce the frequency of the stop band by patterning the inside surfaces of the plates that define the geometry of the gap.

The samples are Perspex plates of thickness $h_p = 5.6$ mm, into which a square array of circular holes (pitch, $\Lambda = 8$ mm, diameter, $d = 2.4$ mm) are drilled. The original ADF sample[9] uses these simple perforated plates. To form the modified structure, referred to as the Helmholtz ADF (HADF), a set of 4 mm wide slots are milled into one side of each plate to a depth of $h_m = 3$ mm. This leaves a square island around each hole of side length $l = 4$ mm. For both the ADF and the HADF samples, the plates are clamped together with the holes in each plate aligned and the plates separated by the gap h_g.

The experimental setup consists of a small loudspeaker (5 cm diameter), which is assumed to be an acoustic

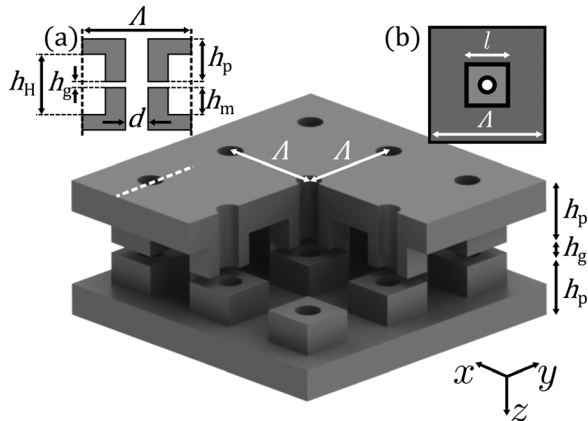a)Author to whom correspondence should be addressed. Electronic mail: a.r.j.murray@exeter.ac.uk

FIG. 1. Schematic of the HADF structure with plate thickness h_p and gap height h_g. The pitch of the hole array is Λ and the hole diameter is d. Rectangular grooves of depth h_m gives a total cavity height of $h_H = 2\,h_m + h_g$. Inset: (a) yz-plane view of the unit cell corresponding to the dashed white line, (b) xy-plane view of the unit cell with island side-length $2\,l$.

point-like source, located at the 1 m focus of a 2 m radius, spherical, concave, aluminum mirrors. Sound waves are collimated by the mirror and directed onto the sample at normal incidence. The transmitted signal is refocused onto a detector located at the 1 m focus of a second identical mirror, which is nominally 3 m away from the primary mirror with the sample located centrally between the mirrors. The frequency-dependent transmittance is determined by taking the ratio of the Fourier transform of the pulse detected after passing through the sample, with the Fourier transform of the unobstructed pulse. The pulse contains frequencies in the range 5 to 30 kHz. Over this range, the Perspex is considered to be a good approximation to a perfectly rigid body.

The experimentally determined transmittance of both the ADF and HADF samples are compared to the predictions of finite element method (FEM) modeling (COMSOL) in Fig. 2. The
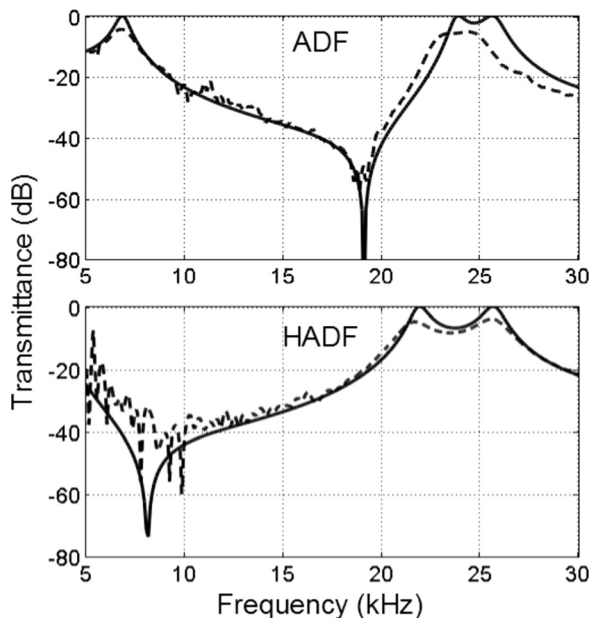

FIG. 2. Plot of experimental transmittance through the ADF (top) and HADF (bottom) structures (dashed line), together with the respective modeled (FEM) transmittance (solid lines). The gap height $h_g = 0.47$ mm.

experimental data for the ADF structure (upper plot, dashed line) shows a clear dip in transmittance at 19 kHz in agreement with the model (solid line). The experimental data for the HADF structure (lower plot, dashed line) shows a minimum in transmittance close to 8 kHz also in agreement with the model (solid line). The free-field wavelength at this minimum is around four times the overall structure thickness and around 5.5 times the array pitch; However, it should be noted that by changing the structure of the gap the exact values of these ratios will be changed. Transmission peaks associated with the pipe resonances of the structure are also observed, however, while the observed frequencies are in the vicinity of the FEM predicted frequencies, there is disagreement and the experimental transmission does not reach unity. This discrepancy is due to the effects of viscous losses that are present within the narrow pipes, which is not accounted for in the FEM modeling shown in Fig. 2.

A Helmholtz resonator consists of a cavity of volume V, and a neck with length L and cross-sectional area A. The resonant frequency is given by[19]

$$f_H = \frac{c}{2\pi}\sqrt{\frac{A}{V \cdot L}}, \tag{1}$$

where c is the speed of sound in the medium (in our case, air). In the plane of the gap between the plates, each unit cell (centered on a hole) consists of a narrower gap surrounded by a wider gap, and hence this new structure functions much like a set of Helmholtz resonators. The volume V is thus $(\Lambda^2 - (l)^2)h_H$ and, allowing for the variation of the cross-section and length of the neck as it runs from the central hole towards the cavity, one may estimate $L = (l - d)/2$ and $A = \pi d h_g$. The effective length and cross-sectional area of the neck are both difficult to specify because of the non-trivial geometry of the described Helmholtz resonator. Suitable choice of the structure's dimensions gives a much lower frequency gap mode than the ADF. Substituting numerical values of V, L, and A for the experimental HADF sample into Eq. (1) gives an estimated resonant frequency of 6.5 kHz for a gap height of $h_g = 0.47$ mm, compared with the experimentally and numerically determined value of 8.0 kHz. The discrepancy is unsurprising given the nontrivial geometry of the patterned gap.

Figure 3 shows the modeled transmittance of the HADF as a function of frequency against gap height. At $h_g = 0$ mm, the data shows the first mode of the structure at 13 kHz, corresponding to fitting a half wavelength between the front and back faces of the HADF, and the second mode at 26 kHz, corresponding to fitting a full wavelength between the front and back faces. When the plates are separated ($h_g > 0$ mm) the second mode [passing through markers (a) and (d) in Fig. 3] is largely unaffected due to the pressure node at the position of the gap. However, the first mode possesses a pressure antinode at the position of the gap and hence couples to the Helmholtz gap resonance—it splits into two distinct branches with frequencies above [passing through markers (b) and (e) in Fig. 3] and below [passing through markers (c) and (f) in Fig. 3] the gap-resonance frequency. It is not immediately apparent that both these modes originate from the
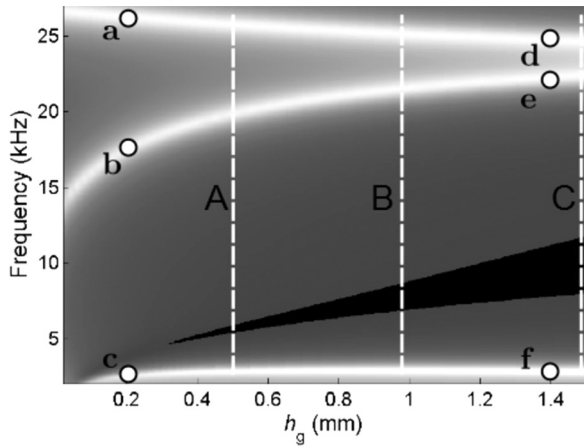
FIG. 3. Grayscale plot of modeled transmittance through the HADF structure as a function of the gap height h_g. White indicates total transmission and black indicates less than $-46\,\text{dB}$ transmission. Markers (a)–(f) correspond to the plots in Fig. 4. The dashed lines (A), (B), and (C) correspond with the experimental data in Fig. 5.

fundamental mode as will be discussed later. As the gap height h_g increases, the system tends towards two isolated plates (i.e., two sets of 6 mm long pipes) and the higher-frequency branch of the first mode converges on the second mode.

Both branches of the first mode correspond to a phase difference of π between the front and back faces; the second mode corresponds to a phase difference of 2π. This can be seen in Fig. 4 which shows the pressure profiles of these modes for $h_g = 0.2\,\text{mm}$ [images (a) (second mode), (b) (upper branch of first mode), and (c) (lower branch of first mode) correspond with markers (a), (b), and (c) in Fig. 3] and for $h_g = 1.4\,\text{mm}$ [images (d) (second mode), (e) (upper

branch of first mode), and (f) (lower branch of first mode) correspond with markers (d), (e), and (f) in Fig. 3]. The second order mode [Figs. 4(a) and 4(c)] achieves an overall phase difference of 2π between the front and back faces of the HADF without experiencing a significant frequency shift. A slight decrease in frequency at larger gap sizes is simply explained by the increased distance between the front and back faces. The upper branch of the first mode [Figs. 4(b) and 4(e)] corresponds to fitting a shorter wavelength into the structure while maintaining an overall phase difference of π between the front and back faces by coupling to the gap resonance; the lower branch conversely corresponds to fitting a significantly longer wavelength into the structure while maintaining [Fig. 4(c) and 4(f)] an overall phase difference of π between the front and back faces, again through coupling to the gap resonance. In fact for the lower-frequency branch there is negligible phase shift through the plate holes and so, within each unit cell, the entire system behaves as a Helmholtz resonator whose neck is formed by the plate holes acting in parallel. This explains why the lower frequency branch in Fig. 3 shows little variation with gap height h_g over most of the range—the resonance frequency [Eq. (1)] depends only on the cavity volume V (see above), whose variation with h_g is small. Regarding the splitting of the first mode into two branches, the lower branch, at a frequency lower than that of the gap resonance, exhibits unusual behavior (see Fig. 3) in that it originates at zero frequency. This is a consequence of the gap-resonance frequency tending to zero as $h_g \rightarrow 0$, as can be seen both from Eq. (1) and from the modeled behavior of the stop-band (the black region in Fig. 3). The lower branch can only exist below the stop band and hence appears to also originate from zero frequency.

III. EXPERIMENTAL RESULTS

Figure 5 shows experimental data (dashed lines) for gap heights (a) $h_g = 0.47\,\text{mm}$, (b) $h_g = 0.94\,\text{mm}$, and
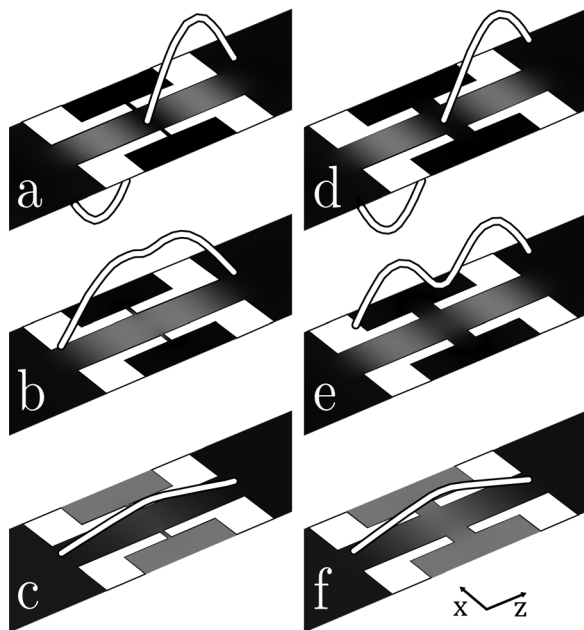

FIG. 4. Grayscale time-averaged pressure maps for the HADF structure [see Fig. 1(a)] corresponding to markers (a)–(f) in Fig. 3. White indicates high pressure amplitude and black indicates low pressure amplitude. Each map has been overlaid with a line profile of the instantaneous pressure through the center of the hole at the phase where the peak amplitude is at a maximum.

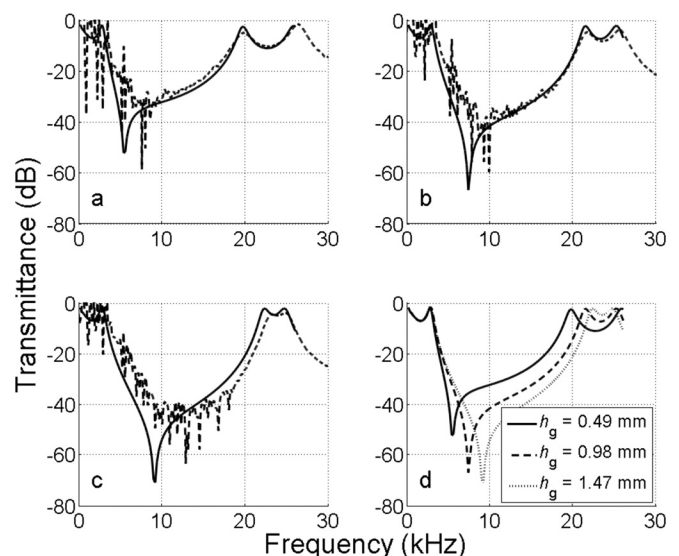FIG. 5. Plots (a)–(c) show experimental (dashed line) and modeled (solid line) data for the HADF structure with gaps of $h_g = 0.49$, 0.98, and 1.47 mm, respectively [see also Fig. 3, lines (A), (B), and (C)]. Plot (d) combines the modeled data from (a)–(c) for direct comparison.

(c) $h_g = 1.47$ mm along with the respective modeling (solid lines). The expected positions of the acoustic stop-band are clearly seen as sharp troughs in the modeled data. Transmission peaks associated with the excitation of pipe modes are also observed in both the experimental and modeled data. Unlike in Fig. 2, the modeled and experimental data show much better agreement. The agreement is due to the inclusion of the effects of viscous losses within the pipes and the gap region, which were not included previously. Discrepancies between the experimental and modeled data are now attributed to variations in the dimensions of the experimental structure. Most notably, the frequency of the stop band in the experimental data is slightly higher than that of the modeled data. This is attributed to the average gap size across the structure being slightly larger than the measured value used for the model. Further evidence of this is provided by observing the separation in frequency of the upper branch of the fundamental mode and the second mode; these modes converge as the gap size is increased. Figure 5(c) shows the experimentally obtained mode separation being considerably smaller than the mode separation in the model, which suggests that the average gap size is larger than the modeled value of $h_g = 1.47$ mm.

The stop band frequencies corresponding with each gap height are in agreement with the square-root dependence suggested by Eq. (1). It is apparent that as the gap height is reduced, the width of the stop band decreases. This is clearly seen in Fig. 5(d) where the three sets of modeled data are plotted together. For convenience, we define the width of the stop band from the points of -46 dB, corresponding to 0.5% transmission. This width for a 0.47 mm gap is 0.7 kHz (12% of the stop band frequency) while for a 0.94 mm gap and for a 1.41 mm gap the widths are 2.3 kHz (30% of the stop band frequency) and 4.3 kHz (46% of the stop band frequency), respectively. The Q-factor of a Helmholtz resonator goes as $A^{-1.5}$ in the lossless regime[11] [Eq. (2)] so it is unsurprising that the width of the stop band decreases as the gap height is reduced. The observed reduction is a closer fit to a A^{-1} dependence which is likely due to the non-trivial geometry of the structure and the reality of viscous losses within the narrow neck,

$$Q = 2\pi \sqrt{V\left(\frac{L}{A}\right)^3}. \quad (2)$$

The described structure has not been optimized to produce a very low frequency stop-band. From Eq. (1) there are three parameters governing the frequency of the Helmholtz resonance, which defines the stop-band.

(1) The volume V can be trivially increased by milling deeper slots into the plates.
(2) For a fixed pitch the product of V and L can be maximized by appropriate choice of l. For a simple Helmholtz resonator governed by Eq. (1) this is a trivial task. Due to the more complicated geometry of the HADF it is difficult to determine what the neck length L is for a given l and hence where the optimum choice of l lies.

(3) The neck cross-section A can be varied by changing the gap h_g between the plates as was discussed. A reduction in h_g lowers the frequency of the stop-band, and from Eq. (2) it can be seen that the Q of the Helmholtz resonance will simultaneously increase leading to a much narrower stop band.

IV. SUMMARY

We have presented results from a simple modification of the ADF geometry which significantly reduces the fundamental stop band frequency of the structure. The introduction of an orthogonal pair of grooves within the gap between the plates causes the gap to respond like an array of Helmholtz resonators which provides the lower frequency response. The lower frequency stop band improves the viability of the HADF for use as a thin and lightweight sound screening device; however, there is a penalty in that the lower stop band frequency also introduces a transmission resonance at a frequency lower than the stop band itself.

[1]T. W. Ebbesen, H. J. Lezek, H. F. Ghaemi, T. Thio, and P. A. Wolff, "Theory of extraordinary optical transmission through sub-wavelength hole arrays," Nature **391**, 667–669 (1998).
[2]H. A. Bethe, "Theory of diffraction by small holes," Phys. Rev. **66**, 163–182 (1944).
[3]J. Christensen, L. Martin-Moreno, and F. J. Garcia-Vidal, "Theory of resonant acoustic transmission through sub-wavelength apertures," Phys. Rev. Lett. **101**, 014301 (2008).
[4]Y. Zhou, M. Lu, L. Feng, X. Ni, Y. Chen, Y. Zhu, S. Zhu, and N. Ming, "Acoustic surface evanescent wave and its dominant contribution to extraordinary acoustic transmission and collimation of sound," Phys. Rev. Lett. **104**, 164301 (2010).
[5]G. D'Aguanno, K. Q. Le, R. Trimm, A. Alu, N. Mattiucci, A. D. Mathias, N. Akozbek, and M. J. Bloemer, "Broadband metamaterial for non-resonant matching of acoustic waves," Sci. Rep. **2**, 340 (2012).
[6]H. Estrada, P. Candelas, A. Uris, F. Belmar, F. J. Garcia de Abajo, and F. Meseguer, "Extraordinary sound screening in perforated plates," Phys. Rev. Lett. **101**, 084302 (2008).
[7]Z. Liu and G. Jin, "Acoustic transmission resonance and suppression through double-layer sub-wavelength hole arrays," J. Phys.: Condens. Matter **22**, 305003 (2010).
[8]J. Christensen, L. Martin-Moreno, and F. J. Garcia-Vidal, "All-angle blockage of sound by an acoustic double-fishnet metamaterial," Appl. Phys. Lett. **97**, 134106 (2010).
[9]Z. Liu, X. Zhang, Y. Mao, Y. Y. Zhu, Z. Yang, C. T. Chan, and P. Sheng, "Locally resonant sonic materials," Science **289**, 1734–1736 (2000).
[10]Z. Yang, H. M. Dai, N. H. Chan, G. C. Ma, and P. Sheng, "Acoustic metamaterial panels for sound absorption in the 50–1000 Hz regime," Appl. Phys. Lett. **96**, 041906 (2010).
[11]C. J. Naify, C. Chang, G. McKnight, and S. R. Nutt, "Scaling of membrane-type locally resonant acoustic metamaterial arrays," J. Acoust. Soc. Am. **132**, 2784–2792 (2012).
[12]J.-P. Groby, O. Dazel, and A. Duclos, "Enhancing the absorption coefficient of a backed rigid frame porous layer by embedding circular periodic inclusions," J. Acoust. Soc. Am. **130**, 3771–3780 (2011).
[13]C. Lagarrigue, J. P. Groby, V. Tournat, and O. Dazel, "Absorption of sound by porous layers with embedded periodic arrays of resonant inclusions," J. Acoust. Soc. Am. **134**, 4670–4680 (2013).

J. Acoust. Soc. Am., Vol. 136, No. 3, September 2014

Murray et al.: Helmholtz double fishnet   983

[14]W. M. Robertson and J. F. Rudy III, "Measurement of acoustic stop bands in two-dimensional periodic scattering arrays," J. Acoust. Soc. Am. **104**, 694–699 (1998).

[15]L. Sanchis, F. Cervera, J. Sánchez-Dehesa, J. V. Sánchez-Perez, C. Rubio, and R. Martínez-Sala, "Reflectance properties of two-dimensional sonic band-gap crystals," J. Acoust. Soc. Am. **109**, 2598–2605 (2001).

[16]A. Gupta, K. M. Lim, and C. H. Chew. "A quasi two-dimensional model for sound attenuation by the sonic crystals," J. Acoust. Soc. Am. **132**, 2909–2914 (2012).

[17]J. S. Bell, I. R. Summers, A. R. J. Murray, E. Hendry, J. R. Sambles, and A. P. Hibbins, "Low acoustic transmittance through a holey structure," Phys. Rev. B **85**, 214305 (2012).

[18]A. R. J. Murray, E. Hendry, I. R. Summers, J. R. Sambles, and A. P. Hibbins, "Control of the stop band of an acoustic double fishnet," J. Acoust. Soc. Am. **134**, 1754–1759 (2013).

[19]L. E. Kinsler, A. R. Frey, A. B. Coppens, and J. V. Sanders, *Fundamentals of Acoustics*, 3rd ed. (Wiley, New York, 2000), pp. 225–227.